Neuronal Androgen Receptor Regulates Insulin Sensitivity via Suppression of Hypothalamic NF-κB–Mediated PTP1B Expression

I-Chen Yu,[1,2] Hung-Yun Lin,[1] Ning-Chun Liu,[1] Janet D. Sparks,[1] Shuyuan Yeh,[1] Lei-Ya Fang,[1] Lumin Chen,[1,3] and Chawnshang Chang[1,3]

Clinical investigations highlight the increased incidence of metabolic syndrome in prostate cancer (PCa) patients receiving androgen deprivation therapy (ADT). Studies using global androgen receptor (AR) knockout mice demonstrate that AR deficiency results in the development of insulin resistance in males. However, mechanisms by which AR in individual organs coordinately regulates insulin sensitivity remain unexplored. Here we tested the hypothesis that functional AR in the brain contributes to whole-body insulin sensitivity regulation and to the metabolic abnormalities developed in AR-deficient male mice. The mouse model selectively lacking AR in the central nervous system and AR-expressing GT1-7 neuronal cells were established and used to delineate molecular mechanisms in insulin signaling modulated by AR. Neuronal AR deficiency leads to reduced insulin sensitivity in middle-aged mice. Neuronal AR regulates hypothalamic insulin signaling by repressing nuclear factor-κB (NF-κB)–mediated induction of protein-tyrosine phosphatase 1B (PTP1B). Hypothalamic insulin resistance leads to hepatic insulin resistance, lipid accumulation, and visceral obesity. The functional deficiency of AR in the hypothalamus leads to male mice being more susceptible to the effects of high-fat diet consumption on PTP1B expression and NF-κB activation. These findings suggest that in men with PCa undergoing ADT, reduction of AR function in the brain may contribute to insulin resistance and visceral obesity. Pharmacotherapies targeting neuronal AR and NF-κB may be developed to combat the metabolic syndrome in men receiving ADT and in elderly men with age-associated hypogonadism. ***Diabetes*** **62:411–423, 2013**

Prostate cancer (PCa), one of the most frequently diagnosed malignancies in men in the Western world, represents 25% of cancers among men (1). Androgen deprivation therapy (ADT) is the fundamental management for men with locally confined, advanced, and metastatic PCa to suppress the functions of androgen/androgen receptor (AR) signaling using AR antagonists in conjunction with bilateral orchiectomy. Although ADT is the frontline and effective treatment for PCa, the resulting profound hypogonadism has adverse effects associated with metabolic syndrome and cardiovascular-related mortality (2–4). The accumulation of visceral adiposity during a short-term ADT period is associated with increasing insulin levels, which may be an initiating event leading to metabolic dysregulation (5). Men receiving long-term ADT treatment develop significant insulin resistance, hyperglycemia, and cardiovascular mortality compared with the non-ADT and control groups (2,6,7). These studies highlight the increased risk of metabolic syndrome, cardiovascular disease, and type 2 diabetes in men with PCa receiving ADT.

Consistent with the relationship of decreased AR function with metabolic syndrome are previous studies demonstrating that genetic inactivation and global loss of AR (AR knockout [ARKO]) lead to the development of excess adiposity associated with insulin resistance and altered glucose homeostasis (8). As testosterone replacement cannot reverse the metabolic abnormalities and insulin resistance observed in ARKO male mice, this suggests that AR is critical in mediating the effects of androgens to regulate glucose and lipid homeostasis in males. Moreover, male mice with hepatic-specific AR deletion more rapidly develop hepatic steatosis and insulin resistance induced by high-fat diet (HFD) feeding and age (9). These findings provide strong evidence that functional deficiency of AR leads to insulin resistance in male mice.

Compelling evidence is mounting that the brain is an insulin target organ that plays a key role in glucose homeostasis and energy balance. Central insulin resistance is suggested to participate critically in the pathophysiology of obesity, type 2 diabetes, and related metabolic disorders (10–12). Differential sensitivity to exogenous insulin in the male and female central nervous system has been observed in animals and humans (13–15). Male rats decrease their food intake and body weight when receiving intracerebroventricular insulin administration, whereas female rats remain largely unaffected (13). Analogous studies have been reported for humans using an intranasal route of insulin delivery, showing that men, but not women, decrease body weight and body fat after 8 weeks of intranasal insulin (14). Moreover, a single dose of insulin reduces food intake in men, but not in women (15).

Although the development of insulin resistance in different tissues may be temporally and mechanistically distinct, there are complicated interorgan communications among the various sites of insulin action. For example, defective hypothalamic insulin signaling is able to promote hepatic insulin resistance in brain-specific insulin receptor (IR) knockout mice (10). Restoration of liver insulin signaling in the whole body of the IR knockout mice fails to normalize insulin action to suppress hepatic glucose production, further supporting the importance of the hypothalamus in insulin signaling (16).

From the [1]George Whipple Laboratory for Cancer Research, Departments of Pathology and Urology, and the Wilmot Cancer Center, University of Rochester Medical Center, Rochester, New York; the [2]Interdepartmental Graduate Program of Neuroscience, University of Rochester Medical Center, Rochester, New York; and the [3]Sex Hormone Research Center, China Medical University/Hospital, Taichung, Taiwan.
Corresponding author: Chawnshang Chang, chang@urmc.rochester.edu.
Received 12 February 2012 and accepted 1 August 2012.
DOI: 10.2337/db12-0135
This article contains Supplementary Data online at http://diabetes.diabetesjournals.org/lookup/suppl/doi:10.2337/db12-0135/-/DC1.

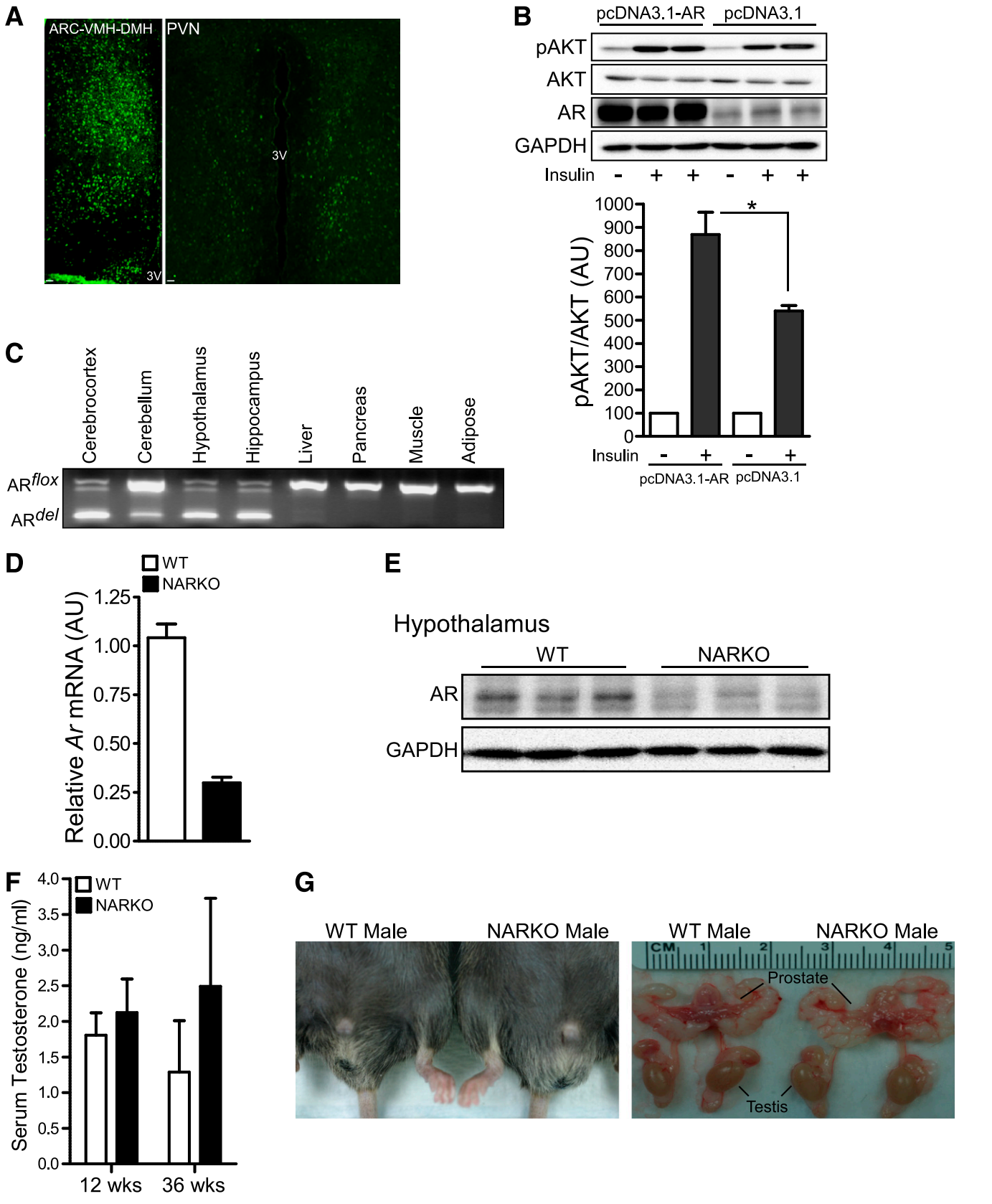

FIG. 1. Central nervous system–specific AR deletion. *A*: Immunohistochemistry with anti-AR antibody in the hypothalamus of adult male brain. ARC, arcuate nucleus; DMH, dorsomedial hypothalamus; PVN, paraventricular nucleus; 3V, the third ventricle; VMH, ventromedial hypothalamus. Bar, 50 μm. *B*, *top*: N2A cells plated on a six-well culture plate were transiently transfected with the pcDNA3.1-AR construct to overexpress AR or with its control vector pcDNA3.1. After 48 h, the N2A cells were subjected to serum starvation overnight followed by 0.1 nmol/L insulin stimulation for 30 min. The AKT phosphorylation response to insulin stimulation was analyzed by anti-pSer473 AKT antibody in harvested cell lysates. Immunoblotting with anti-AR antibody was examined to detect AR expression levels, and immunoblotting with anti–glyceraldehyde-3-phosphate dehydrogenase (GAPDH) was examined to detect equal amounts of cell lysate loading. *B*, *bottom*: Ratios of pAKT to total AKT were statistically

We hypothesized that functional AR in the brain may contribute to insulin sensitivity in the male brain and to the metabolic abnormalities in ARKO male mice, which may implicate the insulin resistance developed in men with PCa undergoing ADT. We used neuronal-specific AR knockout (NARKO) mice to directly determine the function of brain AR in insulin sensitivity. Our results demonstrate that neuronal AR deficiency results in dysregulation of central insulin action and abnormalities in whole-body glucose homeostasis. Loss of neuronal AR leads to increased activation of hypothalamic nuclear factor-κB (NF-κB), which induces the expression of protein-tyrosine phosphatase 1B (PTP1B), which interferes with hypothalamic insulin signaling. Impaired hypothalamic insulin signaling contributes to increased hepatic glucose production, systemic insulin resistance, and excessive fat deposition, further supporting the critical role of functional brain AR in restraining the development of obesity.

RESEARCH DESIGN AND METHODS

Animals and reagents. All animal study protocols were reviewed and approved by the Animal Care and Use Committee of the University of Rochester Medical Center, in accordance with National Institutes of Health guidelines. The floxAR mice, targeting vector construction, and chimera founder generation have been described previously (17). The synapsin I–Cre mice were provided by Dr. David Rempe (University of Rochester) and bred in a C57BL/6J background. NARKO mice were identified by genomic DNA PCR, as described previously (17). Animals were housed in pathogen-free facilities, maintained on a 12-h light-dark cycle schedule, and had access to standard laboratory chow (no. 5010, Laboratory Diet; PMI Nutrition International) and water ad libitum. The mouse neuronal cell line, Neuro-2A (N2A) was obtained from American Type Culture Collection (Manassas, VA). The hypothalamic GT1-7 cell line was provided by Dr. Pamela Mellon (University of California San Diego, San Diego, CA).

Biochemical analysis. Fasting blood samples were taken from mice 16–18 h after withdrawal of food. Blood glucose was measured using a glucometer (One Touch Ultra; LifeScan). Serum insulin and leptin were determined using insulin and leptin ELISA kits (Crystal Chem) according to the manufacturer's protocol. Serum triglyceride was determined by GPO-Trinder assay (Sigma-Aldrich). Serum free fatty acid was measured using a NEFA-Kit-U (Wako). Serum testosterone was determined using an ELISA kit (Diagnostic Systems Laboratories). Tissue triglyceride content was determined in the extracts from 50–100 mg fresh, frozen livers as described previously (9).

Insulin and pyruvate tolerance tests. Insulin tolerance tests were performed on 6-h fasted mice after intraperitoneal injection of 1 unit/kg body weight recombinant bovine insulin (Sigma Aldrich). Blood glucose concentrations were determined at 0, 15, 30, 45, 60, and 90 min after insulin administration. Blood glucose was measured, and the percentage of reduction in blood glucose was compared with the zero time within groups. For the pyruvate tolerance test (PTT), after an 18-h fast, mice received an intraperitoneal injection of 2 g/kg body weight sodium pyruvate (Sigma-Aldrich). Blood glucose concentrations were measured at time points indicated after injection.

RNA extraction and real-time quantitative PCR analysis. Total RNA was prepared from cells or tissues with TRIzol (Invitrogen) according to the manufacturer's instructions. cDNA synthesis was carried out by RT-PCR with Superscript RNase H-reverse transcriptase and cDNA cycle kit (Invitrogen) using 4 μg total RNA according to the manufacturer's instructions. Expression levels of RNA were determined by quantitative real-time PCR performed in an iCycler real-time PCR amplifier (Bio-Rad Laboratories) using iQ SYBR Green Supermix reagent (Invitrogen). The relative copy number of *Gapdh* RNA was quantified and used for normalization. The $\Delta\Delta C_T$ method was used to calculate relative differences between wild-type (WT) and knockout mice.

Statistical analysis. Data are presented as mean ± SEM. Differences between two means were assessed by unpaired, two-tailed Student *t* test. Data involving more than two means were evaluated by one-way ANOVA followed by Tukey post hoc tests (SigmaStat [SyStat] and GraphPad Prism [GraphPad Software, Inc.]). *P* values <0.05 are considered statistically significant.

RESULTS

AR modulates insulin signaling in neuronal cells. Immunohistochemical analysis showed that AR was highly expressed within the arcuate nucleus of the hypothalamus, ventromedial hypothalamus, and dorsomedial hypothalamus, while accounting for a relatively small fraction of cells in the paraventricular nucleus (Fig. 1*A*). These results suggested the putative role of AR in the hypothalamus, the critical site of insulin's action on glucose homeostasis in the brain. To address whether AR regulated insulin signaling in neuronal cells, we manipulated AR expression in N2A cells and found that overexpression of AR enhanced insulin-dependent phosphorylation of AKT (Fig. 1*B*). In contrast, knocking down AR expression in N2A cells resulted in decreased insulin-stimulated AKT phosphorylation (Supplementary Fig. 1*A*). To further investigate the role of AR in regulating insulin signaling in neuronal cells in vivo, we generated NARKO mice by crossing floxAR mice with synapsin I–Cre mice (18). Cre-mediated genomic DNA recombination of floxed AR allele was detected in various areas of the brain, including the cerebrocortex, hypothalamus, hippocampus, and, to a relatively less extent, in the cerebellum. In contrast, AR DNA deletion was not detected in peripheral tissues, indicating a restricted AR disruption in the central nervous system (Fig. 1*C*). Disruption of AR in the hypothalamus of NARKO mice was examined using AR mRNA and protein expression analysis (Fig. 1*D* and *E*). NARKO mice exhibited a >85% decrease in AR expression in neurons in the arcuate nucleus of the hypothalamus, ventromedial hypothalamus, dorsomedial hypothalamus, and paraventricular nucleus (Supplementary Fig. 1*B* and *C*). Circulating testosterone levels in NARKO mice were measured and were not statistically different from controls (Fig. 1*F*), supporting our strategy to determine the function of brain AR without the complication of reduced testosterone signaling occurring with global AR deletion. The presence of normal external genitalia and internal reproductive organs in NARKO mice indicated normal androgen action in male sexual development (Fig. 1*G*).

Impaired energy homeostasis and insulin resistance in middle-aged NARKO mice. To determine the importance of neuronal AR deficiency in the regulation of energy homeostasis, we monitored the body weights of NARKO mice and found there was a significant increase beginning at 28 weeks of age and thereafter (Fig. 2*A*). Consistent with the growth curves, NARKO mice at 36 weeks of age had increased visceral adiposity, reflected by enlargement of both epididymal and retroperitoneal fat pads, which was primarily accounted for by the increased size of the adipocytes (Fig. 2*B–D*). These data indicated the development of obesity and impaired energy homeostasis, which was also revealed by changed metabolic parameters

analyzed from three independent experiments. *$P < 0.05$. *C*: Semiquantitative PCR analysis of genomic DNA from various tissues and brain areas of NARKO mice. AR^{flox}, targeted AR locus; AR^{del}, deleted AR locus. *D*: Expression of *Ar* mRNA in the hypothalamus of NARKO mice and their WT littermates at 10–12 weeks of age was determined by quantitative RT-PCR. Data presented as mean ± SEM; *n* = 8–9 mice per genotype. *E*: Tissue lysates from the hypothalamus of NARKO mice and WT littermates at 10–12 weeks of age were immunoblotted with anti-AR antibody to detect AR protein and anti-GAPDH antibody to detect equal amounts of loading. *F*: Levels of circulating testosterone were determined in the serum extracted from young-adult (12 weeks [wks] of age) and middle-aged (36 weeks of age) male NARKO and WT mice. Data presented as mean ± SEM; *n* = 6–9 mice per genotype. *G*: Representative photographs of external and internal genitalia of male NARKO and WT mice at the 12 weeks of age. AU, arbitrary unit. (A high-quality digital representation of this figure is available in the online issue.)

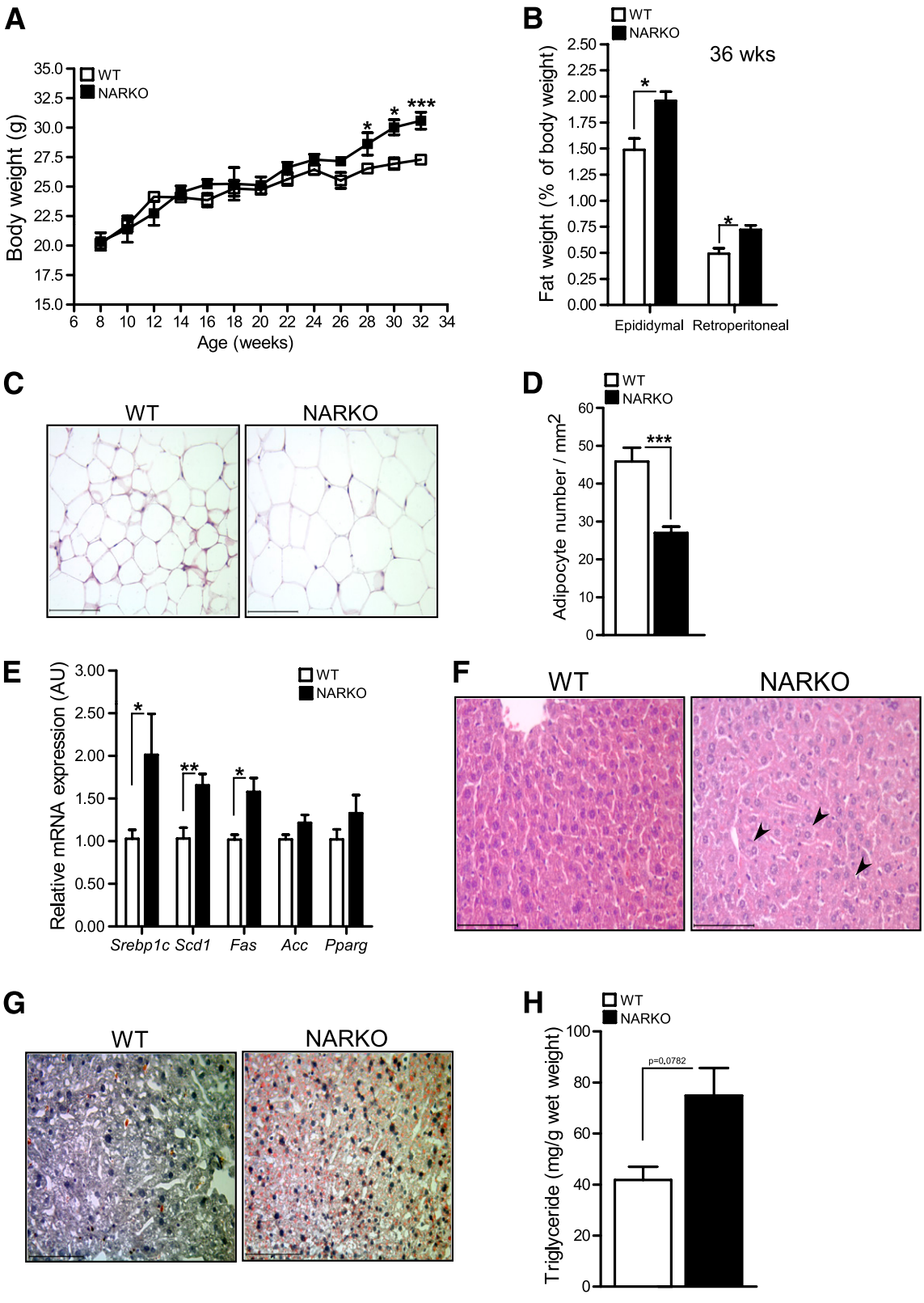

FIG. 2. Visceral obesity, altered peripheral lipid metabolism, and insulin resistance of NARKO mice. *A*: Growth curves of NARKO and WT mice. Animals were fed with normal chow diet. Body weight was measured every 2 weeks from 8 to 32 weeks of age. Data are presented as mean ± SEM. *$P < 0.05$ and ***$P < 0.001$ for NARKO vs. WT; $n = 15$ mice per group. *B*: Fat mass of epididymal and retroperitoneal fat pads isolated from NARKO and WT mice at 36 weeks of age. Data presented as mean ± SEM. *$P < 0.05$ for NARKO vs. WT; $n = 8$–11 mice per group. *C*: Histological analyses of epididymal fat sections from NARKO and WT mice at 36 weeks of age by hematoxylin and eosin (H&E) staining. Bar, 100 μm. *D*: The number of adipocytes was calculated per mm^2 area under microscope field. Data presented as mean ± SEM. ***$P < 0.001$ for NARKO vs. WT; $n = 6$–7 mice per group. *E*: Expression of lipogenic genes *Srebp1c*, stearoyl-CoA desaturase 1 (*Scd1*), fatty acid synthase (*Fas*), acetyl CoA carboxylase (*Acc*), peroxisome proliferator–activated receptor γ (*Pparg*) in the livers of NARKO and WT mice at the 36 weeks of age was analyzed by quantitative RT-PCR. Data presented as mean ± SEM. *$P < 0.05$ and **$P < 0.01$ for NARKO vs. WT; $n = 8$–11 mice per group. *F*: Histological analyses of liver sections from NARKO and WT mice at 36 weeks [wks] of age by H&E staining. Arrowheads indicate lipid vacuoles surrounding the nuclei of hepatocytes.

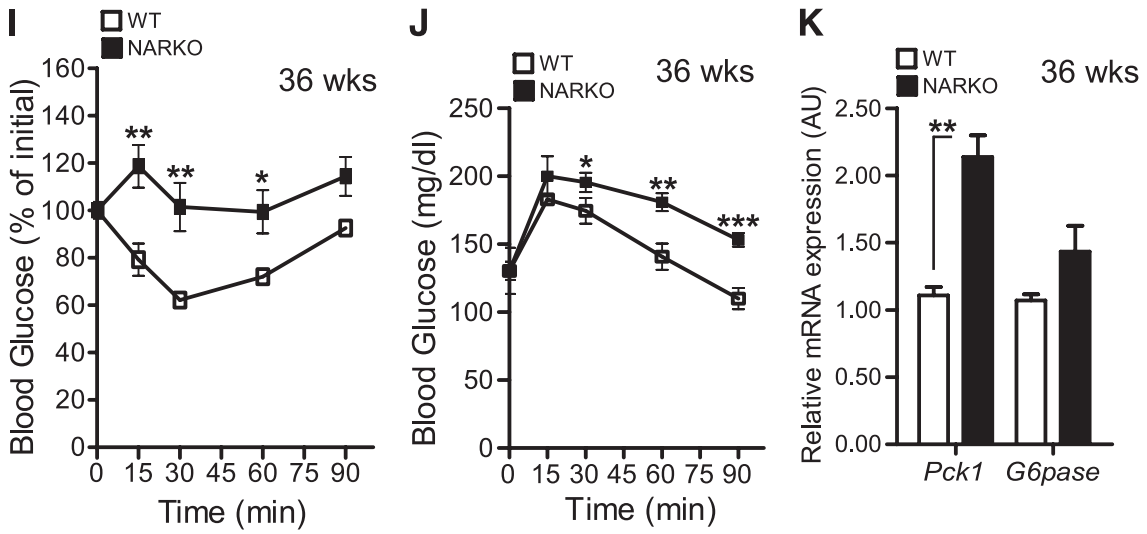

FIG. 2. (*Continued*) Bar, 100 μm. *G*: Histological analyses of liver sections from NARKO and WT mice at 36 weeks of age by Oil Red O staining to detect the presence of lipid droplets. Bar, 100 μm. *H*: Liver triglyceride contents were measured in fresh, frozen livers from 16-h fasted NARKO and WT mice at 36 weeks of age. Data presented as mean ± SEM; *n* = 4–6 mice per group. *I*: Insulin tolerance test (1 unit/kg body weight) was performed in 6-h fasted NARKO and WT mice at 36 weeks of age. Blood glucose was measured at the times indicated after intraperitoneal insulin injection. The percentage of reduction in blood glucose was compared with the zero time within groups. Data presented as mean ± SEM. **P* < 0.05 and ***P* < 0.01 for NARKO vs. WT; *n* = 8–11 mice per group. *J*: PTTs were performed after intraperitoneal pyruvate injection (2 g/kg body weight) in 18-h fasted NARKO and WT mice at 36 weeks of age. Blood glucose was measured at the times indicated after pyruvate injections. Data presented as mean ± SEM. **P* < 0.05, ***P* < 0.01, and ****P* < 0.001 for NARKO vs. WT; *n* = 5–6 mice per group. *K*: Hepatic mRNA expression of phosphoenolpyruvate carboxykinase (*Pck1*) and glucose-6-phosphatase (*G6pase*) in NARKO and WT mice at 36 weeks of age was determined using quantitative RT-PCR. Data presented as mean ± SEM. ***P* < 0.01 for NARKO vs. WT; *n* = 8–11 mice per group. AU, arbitrary unit. (A high-quality digital representation of this figure is available in the online issue.)

in the serum (Table 1). Elevated serum triglycerides and free fatty acid levels suggested excessive hepatic lipid synthesis. Increased expression of hepatic lipogenesis genes sterol regulatory element-binding protein 1c (*Srebp1c*), stearoyl-CoA desaturase 1 (*Scd1*), and fatty acid synthase (*Fas*) in NARKO mice was noted, whereas acetyl CoA carboxylase expression was not significantly elevated (Fig. 2*E*). Hepatic macrovesicular steatosis, although moderate, was noted in the livers of NARKO mice using histological examinations demonstrating numerous intermediate lipid vacuoles surrounding and displacing the nuclei of hepatocytes (Fig. 2*F*). The hepatic lipid accumulation was further revealed by Oil Red O staining to capture lipid droplets within hepatocytes (Fig. 2*G*). Consistent with the histological examination, we detected increased triglycerides in the liver of NARKO mice (Fig. 2*H*).

TABLE 1
Serum metabolic parameters of NARKO and WT mice

	NARKO	WT
Triglyceride (mg/dL)	35.27 ± 1.00*	29.21 ± 1.90
FFAs (mEq/L)	0.41 ± 0.04*	0.22 ± 0.05
Cholesterol (mg/dL)	34.84 ± 2.57	32.62 ± 5.26
Leptin (ng/mL)	1.95 ± 0.20*	0.82 ± 0.34
Blood glucose (mg/dL)		
Fasted	97.67 ± 4.99*	82.00 ± 6.51
Fed	151.61 ± 6.71	147.10 ± 6.10
Insulin (ng/mL)	0.46 ± 0.04*	0.17 ± 0.04
HOMA-IR index	2.10 ± 0.21*	0.68 ± 0.12

Data are means ± SEMs. Fasted (16–18 h) NARKO and WT mice were examined at the age of 36 weeks. The homeostatic model assessment of insulin resistance (HOMA-IR) index was calculated based on fasting blood glucose and insulin levels. FFAs, free fatty acids. **P* < 0.05 for NARKO vs. WT; *n* = 8–11 per group.

Insulin resistance in NARKO mice at 36 weeks of age was suggested by insulin tolerance testing (Fig. 2*I*). The presence of elevated fasting blood glucose and insulin levels provides further evidence to support the notion of insulin resistance (Table 1). Increased gluconeogenesis is a characteristic of insulin resistance and fasting hyperglycemia. PTTs were performed by administration of the gluconeogenic substrate pyruvate to promote gluconeogenesis in the fasting state. NARKO mice exhibited significantly higher blood glucose concentrations at 30, 60, and 90 min after pyruvate administration than control mice (Fig. 2*J*). The glucose area under the curve of PTT showed a 20% increase in NARKO mice, indicating increased gluconeogenesis (data not shown). In fasted NARKO mice, the expression of the hepatic gluconeogenic gene phosphoenolpyruvate carboxykinase (*Pck1*) was also significantly increased, and glucose-6-phosphatase trended upwards (Fig. 2*K*).

Neuronal AR deficiency leads to hypothalamic insulin resistance. Expression of the gluconeogenic genes is tightly controlled by the liver and the brain. Hepatic signal transducer and activator of transcription 3 (STAT3) has been shown to mediate insulin action in the brain to suppress hepatic glucose production, beyond direct activation of insulin signaling in the liver (19,20). We examined the induction of hepatic STAT3 phosphorylation in young and nonobese NARKO mice. The phosphorylation of hepatic STAT3 in control mice was significantly induced by glucose injection as expected. However, STAT3 phosphorylation in livers of NARKO mice was significantly reduced (Fig. 3*A*). These data suggest blunted action of insulin in the brain on the suppression of hepatic glucose production.

Insulin action in agouti-related peptide (AgRP) neurons was demonstrated to be required for suppression of hepatic glucose production (21). Upregulated gene expression of

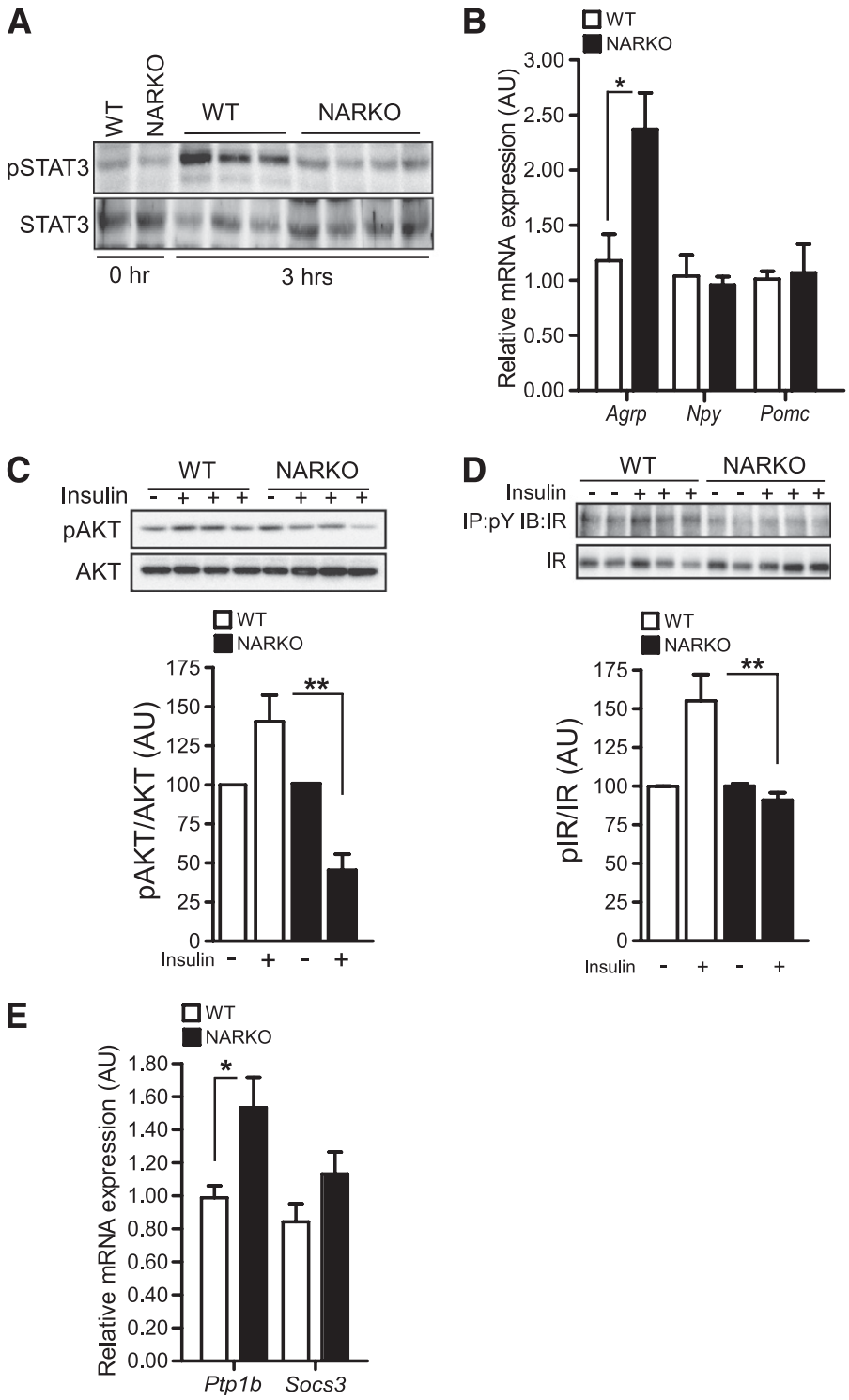

FIG. 3. Impaired hypothalamic insulin signaling. *A*: Immunoblot analysis of the phosphorylation of STAT3 (pSTAT3) versus total STAT3 in the liver at 0 and 3 h after intraperitoneal glucose administration (4 mg/g body weight) in 16-h fasted NARKO mice and their WT littermates. *B*: mRNA expression of hypothalamic neuropeptides, agouti-related peptide (*Agrp*), neuropeptide Y (*Npy*), and pro-opiomelanocortin (*Pomc*), in fasting states (16 h) was determined by quantitative RT-PCR. Data presented as mean ± SEM. **P* < 0.05 for NARKO vs. WT, *n* = 8–11 mice per group. *C*: Immunoblot analysis (*top*) of pAKT vs. total AKT in the hypothalamus of NARKO and WT mice 10 min after intravenous insulin (5 units) infusion. The graph (*bottom*) represents the ratios of phosphoproteins to total proteins. ***P* < 0.01 for NARKO vs. WT. *D*: Tyrosine phosphorylation of hypothalamic IR was detected by immunoprecipitation (IP) with anti-phosphotyrosine (pY) antibody and immunoblotted (IB) with anti-IR antibody at 10 min after intravenous insulin infusion. Total IR proteins were analyzed by immunoblotting (*top*) with input tissue lysates. The graph (*bottom*) represents the ratios of phosphoproteins to total proteins. ***P* < 0.01 for NARKO vs. WT. *E*: mRNA expression of *Ptp1b* and suppressor of cytokine signaling 3 (*Socs3*) in the hypothalamus dissected from 16-h fasted NARO and WT mice was determined by quantitative RT-PCR. Data presented as mean ± SEM. **P* < 0.05 for NARKO vs. WT; *n* = 8–11 mice per group. Animals were examined at 20 weeks of age and matched with similar body weights. AU, arbitrary unit; hr, hour.

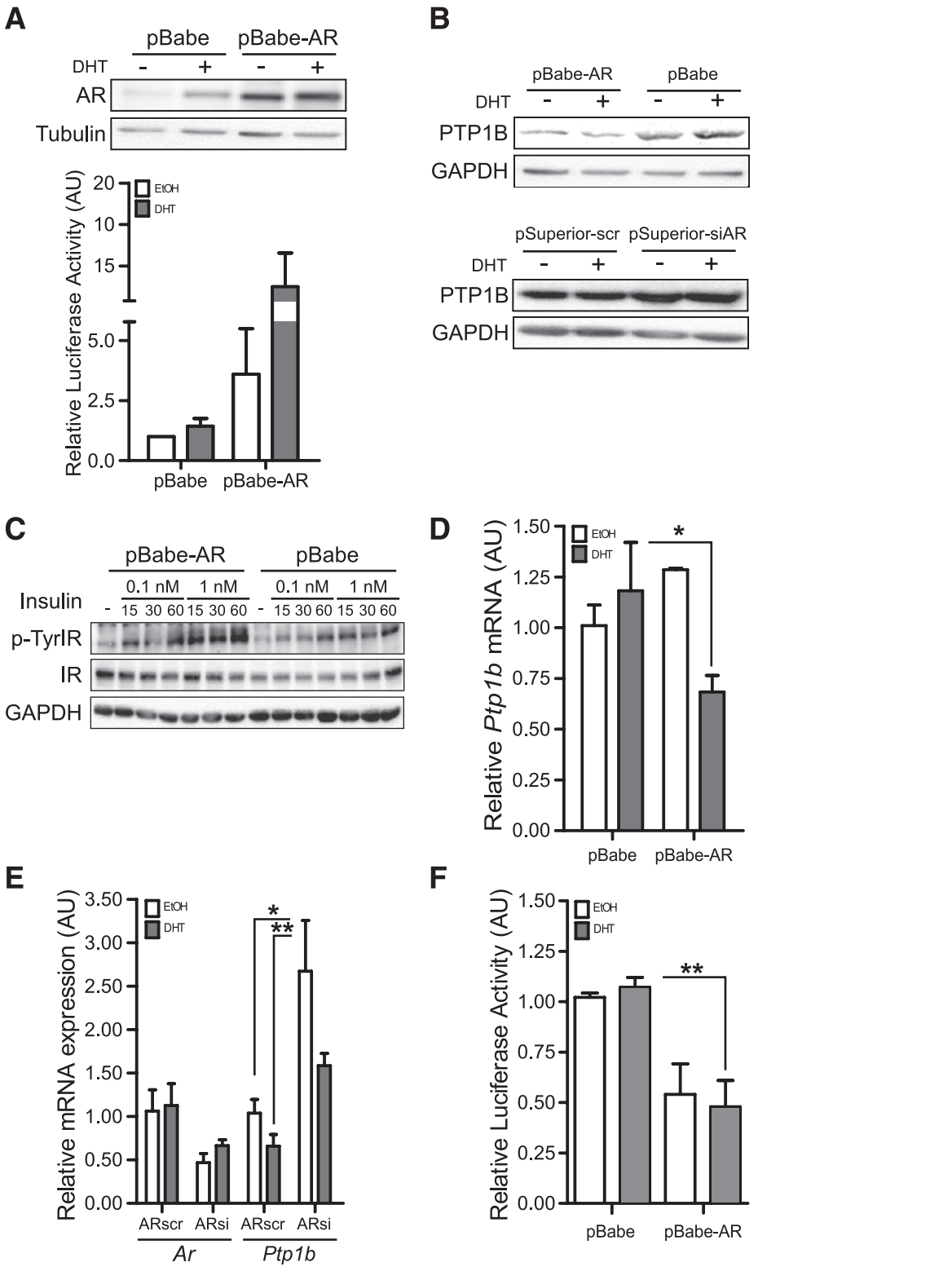

FIG. 4. AR suppresses PTP1B expression in hypothalamic neuron cells. *A*: Immunoblot analysis of AR expression in stably transfected pBabe GT1-7 and pBabe-AR GT1-7 cells with or without 10 nmol/L DHT treatment (*top*). Ethanol (EtOH), the vehicle of DHT, was used as control in cells without DHT treatment. Tubulin was used to detect equal amounts of loading. Mouse mammary tumor virus promoter-luciferase (MMTV-Luc) reporter construct carrying an AR-responsive element was transiently transfected into pBabe GT1-7 and pBabe-AR GT1-7 cells 24 h before treatment. Transfected cells were treated with 10 nmol/L DHT or EtOH control for 24 h, and luciferase activity was measured (*bottom*). *B*: Immunoblot analysis of PTP1B expression in pBabe-AR GT1-7 and pBabe GT1-7 cells with or without 10 nmol/L DHT treatment (*top*) or in pSuperior-scr and pSuperior-siAR transiently transfected GT1-7 cells with or without 10 nmol/L DHT treatment (*bottom*). Cells were treated with 10 nmol/L DHT or ethanol control for 48 h and harvested for analysis. Glyceraldehyde-3-phosphate dehydrogenase (GAPDH) was used to detect equal amounts of loading. *C*: Tyrosine phosphorylation of IR in pBabe-AR GT1-7 and pBabe GT1-7 cells with the presence of 10 nmol/L DHT. Cells were subjected to serum starvation overnight followed by insulin stimulation with 0.1 or 1 nmol/L for 15, 30, or 60 min. IR phosphorylation was analyzed by anti-pTyr1146 IR antibody. *D*: Expression of *Ptp1b* mRNA in pBabe GT1-7 and pBabe-AR GT1-7 cells. *Ptp1b* mRNA was determined by quantitative RT-PCR after 10 nmol/L DHT or EtOH treatment for 24 h. Data presented as mean ± SEM from four independent experiments. *$P < 0.05$

AgRP neuropeptide was noted in the hypothalamus of NARKO mice, further indicating that the dampened action of insulin in the hypothalamus resulted from AR deficiency (Fig. 3*B*). Hypothalamic insulin signaling was examined, and the ability of insulin to stimulate downstream AKT phosphorylation was impaired in the hypothalamus of NARKO mice (Fig. 3*C*). Moreover, NARKO mice exhibited reduced IR phosphorylation in response to insulin administration (Fig. 3*D*). Taken together, these results indicate impaired hypothalamic insulin signaling and hypothalamic insulin resistance in NARKO mice. Intracellular insulin signaling is executed by the tyrosine phosphorylation cascade, and the extent of tyrosyl phosphorylation is regulated by PTPs. While impaired hypothalamic insulin signaling in NARKO mice was observed, we also found an increase of PTP1B expression, a known physiological negative regulator of insulin signaling (Fig. 3*E*). These results suggest that elevated PTP1B levels may contribute to the development of hypothalamic insulin resistance in NARKO mice.

To address whether AR deficiency attenuates hypothalamic insulin signaling through increasing PTP1B-mediated IR dephosphorylation, we stably increased AR expression in murine hypothalamic GT1-7 neuron cells and validated AR expression by transactivation assays (Fig. 4*A*). Overexpression of AR was able to downregulate the expression of PTP1B protein, whereas the expression of PTP1B was slightly increased after knocking down AR expression (Fig. 4*B*). The tyrosine phosphorylation of IR was enhanced in AR-overexpressing cells when stimulated with 1 nmol/L insulin, and it was detected with as low as 0.1 nmol/L insulin in AR-overexpressing cells, compared with control cells (Fig. 4*C*). These data indicate that AR may modulate insulin signaling through regulating PTP1B expression. PTP1B mRNA expression was downregulated by activating AR with its ligand, dihydrotestosterone (DHT) (Fig. 4*D*). In contrast, PTP1B mRNA expression was upregulated when the AR expression was suppressed (Fig. 4*E*). To further address whether AR regulates PTP1B promoter activity, we established a luciferase reporter construct driven by the mouse PTP1B promoter (pGL3-PTP1B) and found that the promoter activity of PTP1B was repressed by AR (Fig. 4*F*). These data suggest that PTP1B expression was regulated by AR-mediated transcriptional suppression.

AR suppresses hypothalamic NF-κB activities. PTP1B expression is induced by inflammation in vivo through NF-κB–mediated transcriptional activation (22). We found that NF-κB induces PTP1B promoter activity in a dose-dependent manner in pBabe GT1-7 control cells, but not in pBabe-AR GT1-7 cells with AR overexpression (Fig. 5*A*). The promoter activity of PTP1B was induced when the AR was knocked down; whereas this induction was blocked by inhibiting NF-κB activity through overexpression of NF-κB inhibitor α (IκBα) (Fig. 5*B*). These results indicate that AR suppresses PTP1B expression by inhibiting NF-κB–mediated transcriptional induction, and that AR can suppress NF-κB activity in hypothalamic neurons. Suppression of the transactivation ability of NF-κB by AR in neuron cells was further observed using reporter constructs responsive to active NF-κB (Fig. 5*C* and Supplementary Fig. 2*A*). Activated hypothalamic NF-κB induced insulin and leptin resistance after HFD consumption was demonstrated to be a critical mediator of chronic overnutrition with energy imbalance and obesity (23). Results showing AR suppression of hypothalamic NF-κB activity suggest that loss of AR suppression may accelerate HFD-induced hypothalamic NF-κB activation.

To further test our hypothesis, we challenged NARKO mice with a short-term HFD feeding paradigm for 14 days and found that HFD significantly induced hypothalamic PTP1B expression in NARKO mice compared with controls where induction was moderate (Fig. 5*D*). The relatively increased hypothalamic NF-κB activation in NARKO mice after short-term HFD was shown by increased NF-κB in the nucleus (Fig. 5*E* and Supplementary Fig. 2*B*). These results indicate a heightened activity of hypothalamic NF-κB responding to HFD challenge in NARKO mice. In addition, an increase of SOCS3 mRNA expression in the hypothalamus of NARKO mice supported the increase of hypothalamic NF-κB activation (Supplementary Fig. 2*C*). The exhibited decrease of hypothalamic insulin receptor substrate 1 (IRS1) protein indicated potentially impaired hypothalamic insulin signaling in NARKO mice under HFD challenge (Supplementary Fig. 2*D*). The short-term HFD challenge hastened activation of hypothalamic NF-κB in young-adult NARKO mice at 10 weeks of age and promoted accelerated weight gain, subtle but significant, compared with controls (Fig. 5*F*). We did not observe a significant increase of food intake in NARKO mice during the short-term HFD feeding period (Fig. 5*G*). Enhanced NF-κB activation may favor a chronic inflammatory status. An increased inflammatory state was noted as more reactive astrogliosis in the hypothalamus and hippocampus of NARKO mice fed chow diets (Supplementary Fig. 2*E*). These results support the notion that decreased AR function may predispose the brain to acute and chronic inflammation via AR regulation of NF-κB activity.

DISCUSSION

Functional AR deficiency contributes to the development of insulin resistance in aging males. In humans, a dose-response relationship between testosterone levels and the odds of developing the metabolic syndrome is observed in men across different ages. Aging men with a 25% decrease of circulating testosterone levels tend to have a twofold increase of metabolic syndrome (24). In rodents, global ARKO male mice start developing insulin resistance at as early as 20 weeks of age (8). However, the mechanisms by which AR in individual organs coordinately regulates insulin sensitivity and contributes to insulin resistance remain largely unexplored. The current study has revealed a previously unrecognized role of neuronal AR in regulating systemic insulin sensitivity. The finding that neuronal AR deficiency is sufficient to reduce insulin sensitivity locally and systemically suggests that the brain neuron may be an initiator of the metabolic consequence resulting from disrupted AR function.

for pBabe-AR vs. pBabe. *E*: *Ptp1b* mRNA in pBabe-AR GT1-7 cells transiently transfected with pSuperior-scr and pSuperior-siAR constructs for 48 h followed by 10 nmol/L DHT or EtOH treatment for another 24 h. *Ar*, AR mRNA; ARscr, pSuperior-scr–transfected cells; ARsi, pSuperior-siAR–transfected cells. Data presented as mean ± SEM from four independent experiments. *$P < 0.05$ and **$P < 0.01$ for pSuperior-siAR vs. pSuperior-scr. *F*: PTP1B gene promoter activity assayed in pBabe GT1-7 and pBabe-AR GT1-7 cells. Cells were transiently transfected with luciferase reporter composed of mouse PTP1B promoter (−1,947 to +183) 24 h before treatment. The transfected cells were treated with 10 nmol/L DHT or EtOH for 24 h, and luciferase activities were measured. Data presented as mean ± SEM from four independent experiments. **$P < 0.01$ for pBabe-AR vs. pBabe. AU, arbitrary unit.

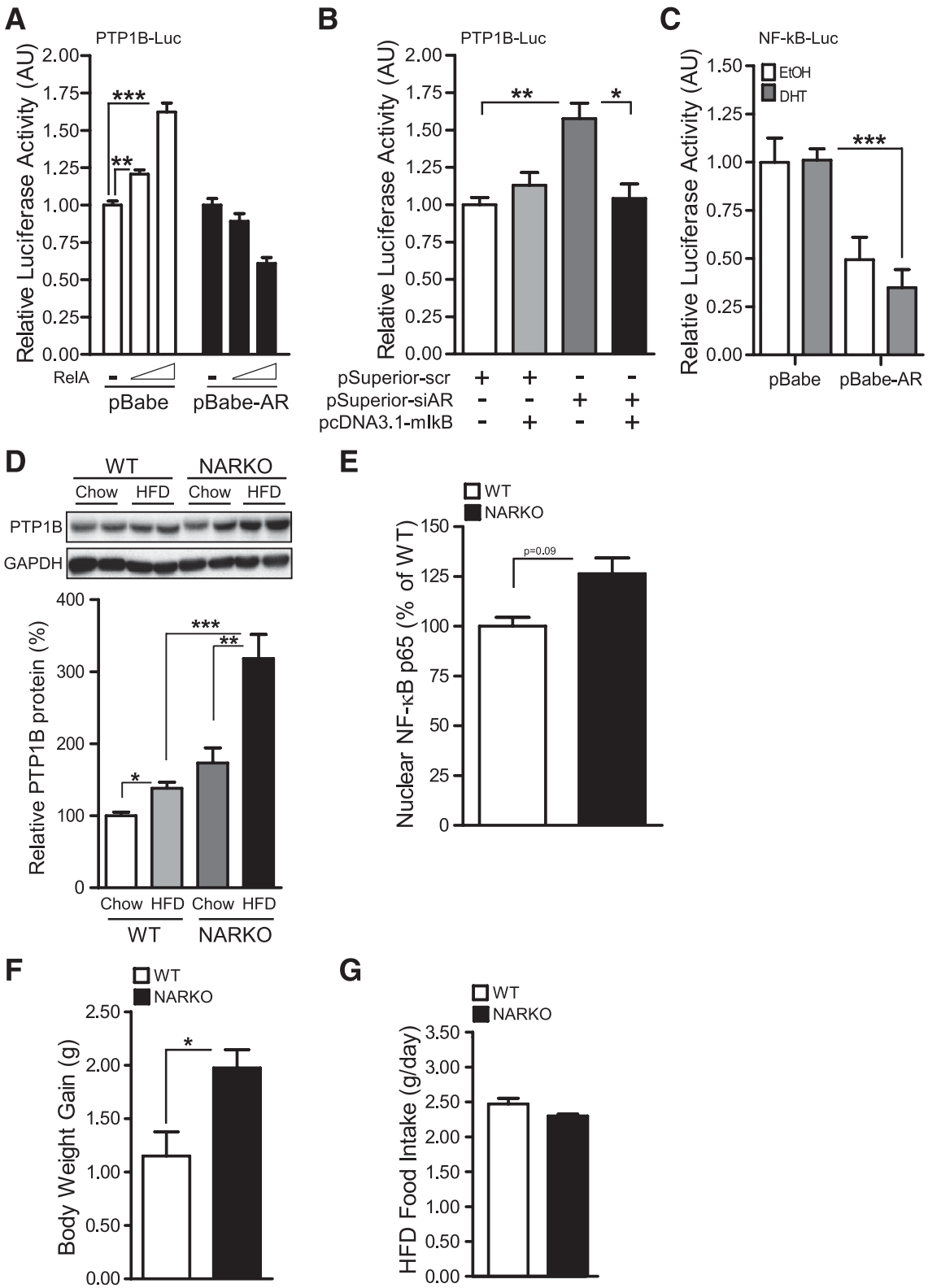

FIG. 5. Loss of AR suppression accelerates HFD-induced hypothalamic NF-κB activation. *A*: NF-κB–induced PTP1B promoter activity in pBabe-AR GT1-7 cells. pBabe GT1-7 and pBabe-AR GT1-7 cells were transiently cotransfected with mouse PTP1B promoter luciferase reporter (PTP1B-Luc) and pcDNA3.1-RelA (RelA) construct (0, 0.2, or 0.4 μg) 24 h before treatment. Plasmid pcDNA3.1 was used as vector control for RelA transfection. Transfected cells were treated with 10 nmol/L DHT for 24 h, and luciferase activities were measured. Dose-dependent RelA expression to activate PTP1B promoter was observed in pBabe GT1-7 cells. Data presented as mean ± SEM from four independent experiments. **$P < 0.01$ and ***$P < 0.001$ for pcDNA3.1-RelA (0.2 and 0.4 μg)–transfected cells vs. vector (pcDNA3.1)-transfected control. *B*: Inhibiting NF-κB activity repressed transactivation of PTP1B promoter induced by knocking down AR expression. pBabe-AR GT1-7 cells were transiently cotransfected with mouse PTP1B promoter luciferase reporter (PTP1B-Luc), pSuperior-scr, pSuperior-siAR, or pcDNA3.1-mIκBα constructs 24 h before treatment with 10 nmol/L DHT for 24 h, and luciferase activities were measured. Plasmid pcDNA3.1 was used as a vector control for mIκBα transfection. Data presented as mean ± SEM from four independent experiments. *$P < 0.05$ and **$P < 0.01$. *C*: NF-κB transactivation activity was suppressed in pBabe GT1-7 and pBabe-AR GT1-7 cells. Cells were transiently transfected with synthetic NF-κB response element luciferase reporter (NF-κB-Luc)

Insulin resistance is strongly associated with sustained inflammatory changes from challenges of nutritional excess (25). Diet-induced metabolic inflammation involves altered intracellular homeostasis, which may atypically trigger NF-κB–mediated inflammation in nonimmune cells to negatively affect intracellular insulin signaling (26,27). Given more susceptibility to intracellular stress, neurons may develop insulin resistance more rapidly than peripheral tissues. This concept is supported by recent findings that hypothalamic insulin resistance is an early event leading to hepatic insulin resistance rather than muscle or adipose tissue insulin resistance under short-term HFD challenge (28). The finding that AR suppresses NF-κB activation at the neuronal level highlights the importance of AR in prevention of the earliest stage of hypothalamic inflammation. The more reactive astrogliosis in the hypothalamus of NARKO mice on a chow diet before development of obesity further suggests that chronic hypothalamic inflammation is induced by functional AR deficiency. Hypothalamic inflammation induced by NF-κB activation can directly promote the expression of hypothalamic PTP1B, which negatively affects insulin signaling within cells (22).

The cross-talk between AR and NF-κB has been shown in PCa cells in vitro, where AR interrupts NF-κB signaling through ligand-dependent induction of IκBα (29). It is also reported that testosterone regulates the inflammatory response through the inhibition of the NF-κB–dependent expression of adhesion molecules and chemokines in human endothelial cells (30). Testosterone inhibition of NF-κB–dependent induction of vascular cell adhesion molecule-1 in human aortic endothelial cells depends on AR function. The suppression effect of testosterone is shown to be completely blocked by the concomitant administration of the AR blocker cyproterone acetate (31). Detailed molecular mechanisms of AR interference with NF-κB remain quite unclear, although induction of IκBα by AR to negatively regulate NF-κB activity was shown in PCa in vivo (32). In the same study, the author also reported DHT-dependent AR function to decrease the NF-κB immunoreactivity in PCa, which provides another mechanism of how AR interrupts NF-κB signaling. In addition, AR/NF-κB interactions or competitive binding to *cis* regulatory DNA elements, between AR and NF-κB, provide different mechanisms of AR interference with NF-κB signaling via ligand-independent or ligand-dependent AR function (33,34).

In the current study, we observed ligand-dependent and ligand-independent AR suppression of NF-κB activity on PTP1B promoter or on the synthetic NF-κB element reporter construct in neuron cells. Induction of IκBα mRNA expression via ligand-dependent AR activation was observed in AR-overexpressed GT1-7 neuron cells (data not shown). We speculated that the interaction between AR and NF-κB might promote stronger interference of NF-κB activation than endogenous AR in a ligand-independent manner in the AR-overexpressed cell culture system. Moreover, posttranslational modifications, such as phosphorylation or acetylation, leading to ligand-independent activation of AR to interrupt NF-κB activity, might contribute to the phenomena we observed. The ligand-independent activation of AR through posttranslational modifications is indeed commonly observed in metastatic PCa cells and contributes to the development of castration-resistant/metastatic PCa (35). Molecular mechanisms of the antagonistic modulation of NF-κB signaling by AR await future studies.

We propose that loss of functional AR in discrete hypothalamic neurons increases the susceptibility to nutrient-induced hypothalamic activation of NF-κB, leading to impairment of insulin action in the brain. Impaired insulin signaling influences the ability of hypothalamic neurons to regulate hepatic gluconeogenesis, through phosphoenolpyruvate carboxykinase. Elevated glucose production in the liver, in turn, leads to the deterioration of hepatic insulin sensitivity and results in insulin resistance. The ensuing insulin resistance induces the hepatic lipogenic regulator Srebp1c and promotes de novo lipogenesis. This sequence of events consequently raises triglyceride levels in the blood and increases the delivery of free fatty acids to adipose tissue, expanding the fat storage in adipocytes and worsening the insulin-resistant state. Moreover, progressively elevated nutrients and free fatty acids in the circulation can further promote hypothalamic NF-κB activation and lead to chronic hypothalamic inflammation (Fig. 6). Therefore, a vicious cycle is set up for disturbing glucose homeostasis and stimulating further insulin secretion from the pancreas. The net result is the classic triad of metabolic syndrome and type 2 diabetes, hyperglycemia, hyperinsulinemia, and hypertriglyceridemia. The consumption of excessive nutrients may accelerate this vicious cycle, as suggested by short-term HFD challenge in AR-deficient animals showing accelerated weight gain, although no obvious increase of food consumption was observed. More studies, including a longer period of HFD feeding, detailed energy expenditure and food intake examinations, and hypothalamic inflammatory pathway dissections, would be needed in the future to answer the remaining questions.

The significance of our findings to human biology closely relates to the metabolic syndrome association with declined testosterone levels via ADT treatment for PCa. Men undergoing ADT have a higher prevalence of metabolic syndrome, with more than half of the men (55%) in the ADT group developing the metabolic syndrome compared with 22% and 20% of men in the non-ADT and control groups, respectively (36,37). Current studies, although by artificially generated neuronal AR deletion in animal models, link the functions of neuronal AR to the hypothalamic insulin signaling of hepatic glucose production. We suggest that ADT treatment may dampen AR function in the hypothalamus at early stages to influence insulin sensitivity. The increase of serum insulin levels observed in short-term ADT, 1 month after the initiation of ADT, is likely to reflect increased insulin secretion to balance the elevation of hepatic glucose production from impaired hypothalamic insulin signaling.

24 h before treatment. Transfected cells were treated with 10 nmol/L DHT or ethanol (EtOH) for 24 h, and luciferase activities were measured. Data presented as mean ± SEM from four independent experiments. ***$P < 0.001$ for pBabe-AR vs. pBabe GT1-7 cells. *D*: Immunoblot analysis (*top*) of hypothalamic PTP1B expression 14 days after HFD feeding. The graph (*bottom*) represents the relative PTP1B proteins normalized with glyceraldehyde-3-phosphate dehydrogenase (GAPDH). *$P < 0.05$; **$P < 0.01$; ***$P < 0.001$. *E*: ELISA evaluation of NF-κB activation in hypothalamic nuclear extracts from NARKO and WT mice after 14 days of HFD feeding. The absorbance at 450-nm wavelength of WT hypothalamic nuclear extracts was set as 100. Data presented as mean ± SEM; $n = 5$ per group. Weight gain (*F*) and food intake (*G*) of NARKO mice and WT littermates at 8 weeks of age after 14 days of HFD feeding. Data presented as mean ± SEM. *$P < 0.05$ for NARKO vs. WT; $n = 6$ per group. AU, arbitrary unit.

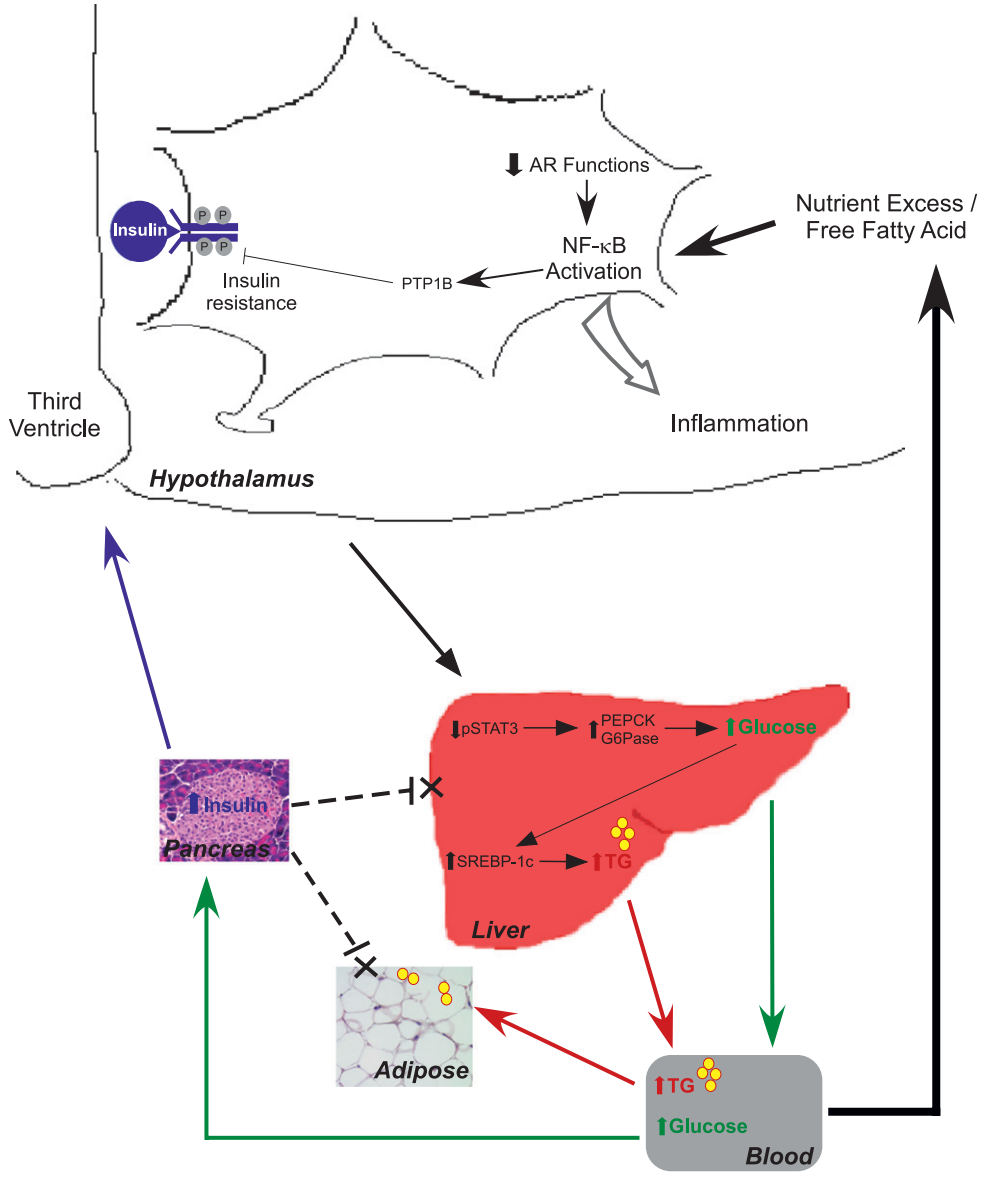

FIG. 6. Schematic diagram of the proposed role of neuronal AR in glucose homeostatic regulation. G6Pase, glucose-6-phosphatase; PEPCK, phosphoenolpyruvate carboxykinase; TG, triglyceride.

Besides ADT treatment, it is clear that aging is associated with the decline in testosterone levels in men (38,39). Longitudinal observations demonstrate that late-onset hypogonadism is a factor in the etiology of metabolic syndrome in elderly men, which can be observed to begin at as early as 40 years of age (24,40,41). Evidence from interventional studies indicates a beneficial effect of testosterone supplementation on the improvement of metabolic manifestations in aging men (42–44). Although showing the benefits of testosterone therapy to ameliorate parameters of the metabolic syndrome, such studies must also take into account the adverse effects of AR overactivation in the prostate with systemic testosterone supplementation. Concerns about long-term effects on the prostate have limited the testosterone supplement as a therapy (45,46). Moreover, men with marked hyperglycemia and insulin resistance after ADT for PCa may not be suitable candidates for testosterone substitution. Correspondingly, selective AR modulators, synthetic ligands that bind to AR and display a tissue-selective activation of AR signaling, may provide a better choice for treatment (47–49). However, more studies are needed to determine whether selective AR modulators specifically targeting neuronal AR can induce meaningful outcomes.

In conclusion, the present findings demonstrate that loss of or decreased functional AR in neurons directly interferes with hypothalamic insulin signaling through enhancement of NF-κB activation. AR suppression of hypothalamic NF-κB activation provides the potential for tissue-selective treatments rather than global testosterone supplementation in PCa patients undergoing ADT. Although challenges still remain, pharmacologically targeting neuronal AR and hypothalamic NF-κB activation may represent a novel strategy to combat obesity and insulin resistance in aging men and patients receiving ADT.

ACKNOWLEDGMENTS

This work was supported by the George Whipple Professorship Endowment, National Institutes of Health grants

CA-155477 and CA-156700, and Department of Health Clinical Trial and Research Center of Excellence Grant DOH99-TD-B-111-004 to China Medical University.

No potential conflicts of interest relevant to this article were reported.

I-C.Y. researched data and wrote the manuscript. H.-Y.L., N.-C.L., and L.-Y.F. researched data. J.D.S. and S.Y. contributed to discussion and reviewed and edited the manuscript. L.C. contributed to discussion. C.C. wrote the manuscript and contributed to discussion. C.C. is the guarantor of this work and, as such, had full access to all the data in the study and takes responsibility for the integrity of the data and the accuracy of the data analysis.

The authors thank Dr. Margot Mayer-Pröschel, Dr. Michael Kerry O'Banion, and Dr. Lisa Opanashuk (University of Rochester Medical Center) for fruitful discussion, critical review, and suggestions. The authors acknowledge Karen Wolf (University of Rochester Medical Center) for manuscript proofreading and preparation.

REFERENCES

1. Jemal A, Siegel R, Ward E, Hao Y, Xu J, Thun MJ. Cancer statistics, 2009. CA Cancer J Clin 2009;59:225–249
2. Basaria S, Muller DC, Carducci MA, Egan J, Dobs AS. Hyperglycemia and insulin resistance in men with prostate carcinoma who receive androgen-deprivation therapy. Cancer 2006;106:581–588
3. Taylor LG, Canfield SE, Du XL. Review of major adverse effects of androgen-deprivation therapy in men with prostate cancer. Cancer 2009; 115:2388–2399
4. Saylor PJ, Smith MR. Adverse effects of androgen deprivation therapy: defining the problem and promoting health among men with prostate cancer. J Natl Compr Canc Netw 2010;8:211–223
5. Smith MR, Lee H, Nathan DM. Insulin sensitivity during combined androgen blockade for prostate cancer. J Clin Endocrinol Metab 2006;91: 1305–1308
6. Saigal CS, Gore JL, Krupski TL, Hanley J, Schonlau M, Litwin MS; and the Urologic Diseases in America Project. Androgen deprivation therapy increases cardiovascular morbidity in men with prostate cancer. Cancer 2007;110:1493–1500
7. Tsai HK, D'Amico AV, Sadetsky N, Chen MH, Carroll PR. Androgen deprivation therapy for localized prostate cancer and the risk of cardiovascular mortality. J Natl Cancer Inst 2007;99:1516–1524
8. Lin HY, Xu Q, Yeh S, Wang RS, Sparks JD, Chang C. Insulin and leptin resistance with hyperleptinemia in mice lacking androgen receptor. Diabetes 2005;54:1717–1725
9. Lin HY, Yu IC, Wang RS, et al. Increased hepatic steatosis and insulin resistance in mice lacking hepatic androgen receptor. Hepatology 2008;47: 1924–1935
10. Brüning JC, Gautam D, Burks DJ, et al. Role of brain insulin receptor in control of body weight and reproduction. Science 2000;289:2122–2125
11. Gelling RW, Morton GJ, Morrison CD, et al. Insulin action in the brain contributes to glucose lowering during insulin treatment of diabetes. Cell Metab 2006;3:67–73
12. Obici S, Feng Z, Karkanias G, Baskin DG, Rossetti L. Decreasing hypothalamic insulin receptors causes hyperphagia and insulin resistance in rats. Nat Neurosci 2002;5:566–572
13. Clegg DJ, Riedy CA, Smith KA, Benoit SC, Woods SC. Differential sensitivity to central leptin and insulin in male and female rats. Diabetes 2003; 52:682–687
14. Hallschmid M, Benedict C, Schultes B, Fehm HL, Born J, Kern W. Intranasal insulin reduces body fat in men but not in women. Diabetes 2004; 53:3024–3029
15. Benedict C, Kern W, Schultes B, Born J, Hallschmid M. Differential sensitivity of men and women to anorexigenic and memory-improving effects of intranasal insulin. J Clin Endocrinol Metab 2008;93:1339–1344
16. Okamoto H, Obici S, Accili D, Rossetti L. Restoration of liver insulin signaling in Insr knockout mice fails to normalize hepatic insulin action. J Clin Invest 2005;115:1314–1322
17. Yeh S, Tsai MY, Xu Q, et al. Generation and characterization of androgen receptor knockout (ARKO) mice: an in vivo model for the study of androgen functions in selective tissues. Proc Natl Acad Sci USA 2002;99: 13498–13503
18. Cohen P, Zhao C, Cai X, et al. Selective deletion of leptin receptor in neurons leads to obesity. J Clin Invest 2001;108:1113–1121
19. Inoue H, Ogawa W, Asakawa A, et al. Role of hepatic STAT3 in brain-insulin action on hepatic glucose production. Cell Metab 2006;3:267–275
20. Ramadoss P, Unger-Smith NE, Lam FS, Hollenberg AN. STAT3 targets the regulatory regions of gluconeogenic genes in vivo. Mol Endocrinol 2009;23: 827–837
21. Könner AC, Janoschek R, Plum L, et al. Insulin action in AgRP-expressing neurons is required for suppression of hepatic glucose production. Cell Metab 2007;5:438–449
22. Zabolotny JM, Kim YB, Welsh LA, Kershaw EE, Neel BG, Kahn BB. Protein-tyrosine phosphatase 1B expression is induced by inflammation in vivo. J Biol Chem 2008;283:14230–14241
23. Zhang X, Zhang G, Zhang H, Karin M, Bai H, Cai D. Hypothalamic IKKbeta/NF-kappaB and ER stress link overnutrition to energy imbalance and obesity. Cell 2008;135:61–73
24. Kupelian V, Hayes FJ, Link CL, Rosen R, McKinlay JB. Inverse association of testosterone and the metabolic syndrome in men is consistent across race and ethnic groups. J Clin Endocrinol Metab 2008;93:3403–3410
25. Hotamisligil GS, Erbay E. Nutrient sensing and inflammation in metabolic diseases. Nat Rev Immunol 2008;8:923–934
26. Cai D, Yuan M, Frantz DF, et al. Local and systemic insulin resistance resulting from hepatic activation of IKK-beta and NF-kappaB. Nat Med 2005;11:183–190
27. Bhatt BA, Dube JJ, Dedousis N, Reider JA, O'Doherty RM. Diet-induced obesity and acute hyperlipidemia reduce IkappaBalpha levels in rat skeletal muscle in a fiber-type dependent manner. Am J Physiol Regul Integr Comp Physiol 2006;290:R233–R240
28. Ono H, Pocai A, Wang Y, et al. Activation of hypothalamic S6 kinase mediates diet-induced hepatic insulin resistance in rats. J Clin Invest 2008; 118:2959–2968
29. Altuwaijri S, Lin HK, Chuang KH, et al. Interruption of nuclear factor kappaB signaling by the androgen receptor facilitates 12-O-tetradecanoylphorbolacetate-induced apoptosis in androgen-sensitive prostate cancer LNCaP cells. Cancer Res 2003;63:7106–7112
30. Norata GD, Tibolla G, Seccomandi PM, Poletti A, Catapano AL. Dihydrotestosterone decreases tumor necrosis factor-alpha and lipopolysaccharide-induced inflammatory response in human endothelial cells. J Clin Endocrinol Metab 2006;91:546–554
31. Hatakeyama H, Nishizawa M, Nakagawa A, Nakano S, Kigoshi T, Uchida K. Testosterone inhibits tumor necrosis factor-alpha-induced vascular cell adhesion molecule-1 expression in human aortic endothelial cells. FEBS Lett 2002;530:129–132
32. Nelius T, Filleur S, Yemelyanov A, et al. Androgen receptor targets NFkappaB and TSP1 to suppress prostate tumor growth in vivo. Int J Cancer 2007;121:999–1008
33. Palvimo JJ, Reinikainen P, Ikonen T, Kallio PJ, Moilanen A, Jänne OA. Mutual transcriptional interference between RelA and androgen receptor. J Biol Chem 1996;271:24151–24156
34. Cinar B, Yeung F, Konaka H, et al. Identification of a negative regulatory cis-element in the enhancer core region of the prostate-specific antigen promoter: implications for intersection of androgen receptor and nuclear factor-kappaB signalling in prostate cancer cells. Biochem J 2004;379:421–431
35. Ai J, Wang Y, Dar JA, et al. HDAC6 regulates androgen receptor hypersensitivity and nuclear localization via modulating Hsp90 acetylation in castration-resistant prostate cancer. Mol Endocrinol 2009;23:1963–1972
36. Braga-Basaria M, Dobs AS, Muller DC, et al. Metabolic syndrome in men with prostate cancer undergoing long-term androgen-deprivation therapy. J Clin Oncol 2006;24:3979–3983
37. Bo JJ, Zhang C, Zhang LH, et al. Androgen deprivation therapy through bilateral orchiectomy: increased metabolic risks. Asian J Androl 2011;13:833–837
38. Harman SM, Metter EJ, Tobin JD, Pearson J, Blackman MR; Baltimore Longitudinal Study of Aging. Longitudinal effects of aging on serum total and free testosterone levels in healthy men. J Clin Endocrinol Metab 2001; 86:724–731
39. Wu FC, Tajar A, Beynon JM, et al.; EMAS Group. Identification of late-onset hypogonadism in middle-aged and elderly men. N Engl J Med 2010; 363:123–135
40. Zitzmann M, Faber S, Nieschlag E. Association of specific symptoms and metabolic risks with serum testosterone in older men. J Clin Endocrinol Metab 2006;91:4335–4343
41. Wang C, Nieschlag E, Swerdloff R, et al. ISA, ISSAM, EAU, EAA and ASA recommendations: investigation, treatment and monitoring of late-onset hypogonadism in males. Int J Impot Res 2009;21:1–8
42. Allan CA, Strauss BJ, Burger HG, Forbes EA, McLachlan RI. Testosterone therapy prevents gain in visceral adipose tissue and loss of skeletal muscle in nonobese aging men. J Clin Endocrinol Metab 2008;93:139–146

43. Schroeder ET, Zheng L, Ong MD, et al. Effects of androgen therapy on adipose tissue and metabolism in older men. J Clin Endocrinol Metab 2004; 89:4863–4872
44. Haider A, Gooren LJ, Padungtod P, Saad F. Improvement of the metabolic syndrome and of non-alcoholic liver steatosis upon treatment of hypogonadal elderly men with parenteral testosterone undecanoate. Exp Clin Endocrinol Diabetes 2010;118:167–171
45. Bhasin S, Cunningham GR, Hayes FJ, et al. Testosterone therapy in adult men with androgen deficiency syndromes: an endocrine society clinical practice guideline. J Clin Endocrinol Metab 2006;91:1995–2010
46. Calof OM, Singh AB, Lee ML, et al. Adverse events associated with testosterone replacement in middle-aged and older men: a meta-analysis of randomized, placebo-controlled trials. J Gerontol A Biol Sci Med Sci 2005; 60:1451–1457
47. Bhasin S, Calof OM, Storer TW, et al. Drug insight: Testosterone and selective androgen receptor modulators as anabolic therapies for chronic illness and aging. Nat Clin Pract Endocrinol Metab 2006;2: 146–159
48. Gao W, Dalton JT. Expanding the therapeutic use of androgens via selective androgen receptor modulators (SARMs). Drug Discov Today 2007; 12:241–248
49. Narayanan R, Mohler ML, Bohl CE, Miller DD, Dalton JT. Selective androgen receptor modulators in preclinical and clinical development. Nucl Recept Signal 2008;6:e010